The First ANZ Young Geotechnical Professionals Conference, Mostyn, Khalili & Small (eds), Feb. 1994, Sydney, Australia

Numerical analysis of a large reinforced soil structure by explicit finite difference codes

D.K.H.Ho
LongMac Associates Pty. Limited, Sydney, NSW, Australia

ABSTRACT: A numerical investigation was carried out to analyse a 22m high "barmat" reinforced soil retaining wall. A computer program, FLAC (Fast Lagrangian Analysis of Continua), was used to perform the analysis. Different failure mechanisms were observed due to the influence of the soil-reinforcement bond stiffness. The significance of the explicit timestepping to a converged solution was also revealed. The computed results were compared with those obtained by the conventional limit equilibrium method.

1 INTRODUCTION

The use of numerical analyses as part of the design process is becoming very common nowadays. Typically they encompass the finite element, finite difference and boundary element methods which have been available to practising engineers for a number of years.

A finite difference codes, FLAC, has been used as a design tool in a number of geotechnical applications. There are a number of advantages of this explicit timestepping algorithm over the implicit program (Itasca, 1991). The calculation routine in the finite difference method involves the timestepping of the solution until the system reaches equilibrium at which time the sum of the net nodal force vector (or the maximum unbalanced force) becomes zero in theory, but for computational purpose, a very small value. Since the equation of motion, which is dynamic in nature, is to be solved, the number of timesteps to obtain a static or quasi-static solution is large in general, even though an adaptive global damping (Cundall, 1982) has been incorporated. The common problems most designers are faced with are: (1) what is the acceptable maximum unbalanced force, (2) what is the number of timesteps required, and (3) when has the system stabilized? Recently, it was reported that different failure mechanisms were observed with timestepping (Itasca-CSIRO, 1993).

In this paper, the results of a large reinforced soil retaining wall analysed by FLAC are presented. One advantage of this model is to identify the development of yield zones which may lead to the potential failure mechanism of such a retaining wall system. The other advantage is the ability to model strain compatibility between the reinforcements and the surrounding soil such that the appropriate soil and reinforcement strengths are mobilised. It is to be noted that the conventional limit state equilibrium analysis assumes the full mobilisation of both components which may not be a true representation of the interaction between the soil and the reinforcement.

In addition, the results of varying the bond stiffness between the soil and the reinforcement are shown.

2 THE REINFORCED SOIL MODELS

2.1 FLAC model

The 22m high wall with 52 layers of steel barmat reinforcements is shown in Figure 1. The wall is to be constructed on an excavated area on the side of a rock slope. Therefore, the wall foundation and the rear of the wall were modelled as fixed boundaries. A plane strain condition was assumed and a surcharge load of 90kPa, 2m away from the edge was applied. The reinforced soil mass was discretised finely in order to minimise the chance of numerical instability. There were about 9000 zones in the model and the aspect ratio within the reinforced zone was unity.

The structural elements of the model comprised the steel facing panels and the barmats. The former was modelled by beam elements while the latter was modelled by cable elements.

The internal stability of the wall was governed by the breaking strength and by the pullout capacity of the reinforcements. The breaking strength was represented simply by the steel's yield stress whilst the pullout resistance was evaluated at each reinforcement level using the overburden stress and a pullout factor as discussed below.

The pullout resistance of this type of reinforcement is derived from the friction between the longitudinal bars and the backfill, and the passive resistance between transverse bars and the backfill. Pullout tests have shown that the pullout resistance is expressed as a function of overburden stress and the bar size. An empirical anchorage factor, A_c, is used to relate the pullout resistance with depth. In this analysis, this factor varied from 40 at the ground surface to 15 at a depth of 6m. Below 6m, A_c remained constant at 15 (NCHRP 1987).

The deformation of the reinforcement is governed by the axial stiffness and the bond stiffness. The effect

of the axial stiffness in reinforced soil wall was reported by Smith et al (1992). However, the influence of the bond stiffness on such a wall system is not certain. In the present analysis, both behaviours were idealised as shown in Figure 2. Three cases of different bond stiffness (each one being 100 times stiffer than the other) were investigated (see Table 1).

The backfill was assumed to be purely frictional and to obey the Mohr-Coulomb yield criterion. No water was assumed to be present in the model. The backfill and the reinforcement properties used in the analyses are summarised in Table 1.

The staged construction of the wall was not modelled. Therefore, compaction was not included in the analyses. A "switch-on" gravity approach was used instead.

2.2 Conventional limit state model

For design purpose, three cases have been analysed using three different sets of strength parameters as shown in Table 1. In case A, the soil was assumed to have mobilised its full shear strength at the same time that the steel had mobilised its working stress. In case B, which was a lower bound case, the steel was more highly stressed than the recommended working stress and the soil strength was not fully mobilised. The last case represented a rather "harsh" situation when the soil strength was only partially mobilised and the steel strength was limited to its working stress.

3 RESULTS AND DISCUSSIONS

In order to examine the stability of the solution with time-stepping, a number of variables namely, the unbalanced force, nodal deformations and zone stresses at pre-selected locations in the wall (see Figure 1) were traced for every 500 steps. Furthermore, the plastic yield zones, grid deformation, and cable tensions were recorded at every 10,000 steps.

The gradual decreases in the unbalanced force for all three cases are shown in Table 2. From this table it can be seen that as the system reaches static equilibrium, the unbalanced force becomes less and less.

The development of tensions with timesteps in the bottom cable and in the highest stressed cable (cable no.7) is shown in Table 3. In all cases, it can be seen that the tension starts from a small value and increases to an almost constant value. The effect of bond stiffness on the cable tension is not obvious. In the case where the bond stiffness is 100 times less than the basic case (case 1), the tension is still increasing at a rate of about 0.2% over 10,000 timesteps.

The traces of the wall crest lateral displacement and the vertical stress inside the reinforced mass at the base of the wall with timesteps for all the cases are shown in Figure 3 and 4 respectively. It appears that in all cases, except case 3, the solution has attained a stable condition after about 80,000 steps.

The "snap shots" of the plastic zones in the backfill for all three cases are shown in Figure 5. In case 1, the potential slip plane "disappeared" after 80,000 steps. In the case where the bond stiffness is stiff, no clear slip surface can be identified but bands of yield zones are observed near the bottom half of the wall. In the case where the bond stiffness is less, two slip surfaces are observed which are consistent with those predicted by the limited equilibrium analyses (see Figure 6).

Although the plastic zones changed with timesteps, the plots of grid deformation gave a clear picture on the failure mechanisms (Figure 7). The exaggerated deformation plot at 10,000 steps is similar to that at 100,000 steps. (Note that the absolute deformation values were different, of course). With the exception of case 2, two slip surfaces are observed for all the other cases. One slip surface begins at the toe of the wall and finishes just behind the surcharge at the top of the wall. The other slip surface starts at the front of the wall at about one third of the wall height, and ends behind the surcharge at the top of the wall. This smaller slip surface is in good agreement with the critical slip surface calculated by the limit equilibrium method.

4. CONCLUSIONS

A large number of timesteps is required to reduce the unbalanced force. However, even though the net unbalanced force is very small, the solution (eg. cable tensions, etc) may not always reach a steady state (although sufficient for practical application).

Different plastic zones are observed with different bond stiffness. It is observed that the bond stiffness determines the yield patterns within the soil.

The plastic zones are observed to be changing with timesteps and it is difficult to identify the development of potential slip planes. But the deformed grid does not change with timesteps, and the slip surface can be defined which is in good agreement with the critical slip based on the conventional limit equilibrium analysis. It is also observed that the plastic zones do not always follow the slip surface as defined from the deformed grid plot.

Futher analyses of the results are needed to determine the influence of the reinforcement bond stiffness. The use of a large strain model could be considered.

REFERENCES

Cundall, P.A. (1982), "Adaptive density-scaling for time-explicit calculations", Proceedings 4th Int. Conf. Numerical Methods in Geomechanics: 23-26.

Itasca (1991), FLAC (Fast Lagrangian Analysis of Continua) Version 3.0. User's Manual. Itasca Consulting Group, Inc.

Itasca-CSIRO (1993), Newsletter No.2, August.

National Cooperative Highway Research Program Report 290 (1987), "Reinforcement of Earth Slopes and Embankments", Transportation Research Board.

Smith, I.M. and Segrestin, P. (1992), "Inextensible reinforcements versus extensible ties - FEM comparative analysis of reinforced or stabilised earth structures", Proceedings of Int. Sym. on Earth Reinforcement Practice, Fukuoka, Kyushu, Japan. 11-13 November.

Table 1 Parameters used in the numerical and the conventional limit state analyses.

FLAC model:

Backfill:	E=45MPa, υ=0.3, γ=25kN/m^3, c'=0kPa & ϕ'=34°.
Face panels:	E=2E8kPa, I=1.302E-9m^4/m width, cross-sectional area=0.0025m^2/m width.
Barmat:	E=2E8kPa, cross-sectional area=function of barmat density. Yield stress=270MPa, pullout capacity=variable.
Case 1:	Bond stiffness=2E3 kN/m/m length
Case 2:	Bond stiffness=2E5 kN/m/m length
Case 3:	Bond stiffness=2E1 kN/m/m length

Limit state model:

Case A:	γ=25kN/m^3, c'=0kPa, ϕ'=34° & steel yield strength=270MPa.
Case B:	γ=25kN/m^3, c'=0kPa, ϕ'=20° & steel yield strength=360MPa.
Case C:	γ=25kN/m^3, c'=0kPa, ϕ'=20° & steel yield strength=270MPa.

Table 2 Variation of unbalanced force with timesteps.

Timestep Number	Case 1		Case 2		Case 3	
	Unbalanced Force (kN)	Percentage of unbalance force (%)	Unbalanced Force (kN)	Percentage of unbalance force (%)	Unbalanced Force (kN)	Percentage of unbalance force (%)
1	18.46	-	18.46	-	18.46	-
10000	0.583	3.158	0.9945	5.387	0.6816	3.692
20000	0.3309	1.793	0.5144	2.787	0.3938	2.133
30000	0.1466	0.794	0.298	1.614	0.1901	1.030
40000	0.3412	1.848	0.07496	0.406	0.08464	0.459
50000	0.04059	0.220	0.04761	0.258	0.06725	0.364
60000	0.02138	0.116	0.02871	0.156	0.07119	0.386
70000	0.01085	0.059	0.01491	0.081	0.05333	0.289
80000	0.005554	0.030	0.007659	0.041	0.06112	0.331
90000	0.001567	0.008	0.004342	0.024	0.02862	0.155
100000	0.0004883	0.003	0.002654	0.014	0.02846	0.154

Table 3 Development of reinforcement tension (kN/m width) with timesteps

Timestep Number	Case 1		Case 2		Case 3	
	Cable 1	Cable 7	Cable 1	Cable 7	Cable 1	Cable 7
1	-	-	-	-	-	-
10000	21.70	57.34	17.59	62.12	20.52	61.62
20000	22.23	58.85	18.82	67.81	20.79	62.69
30000	22.89	60.49	19.65	70.73	20.91	63.22
40000	23.04	60.57	19.76	72.33	20.99	63.57
50000	23.19	61.10	19.76	73.03	21.06	63.85
60000	23.25	61.28	19.95	73.35	21.11	64.04
70000	23.26	61.32	20.04	73.48	21.15	64.12
80000	23.26	61.36	20.07	73.54	21.17	64.18
90000	23.27	61.37	20.09	73.58	21.21	64.33
100000	23.27	61.38	20.10	73.60	21.25	64.46

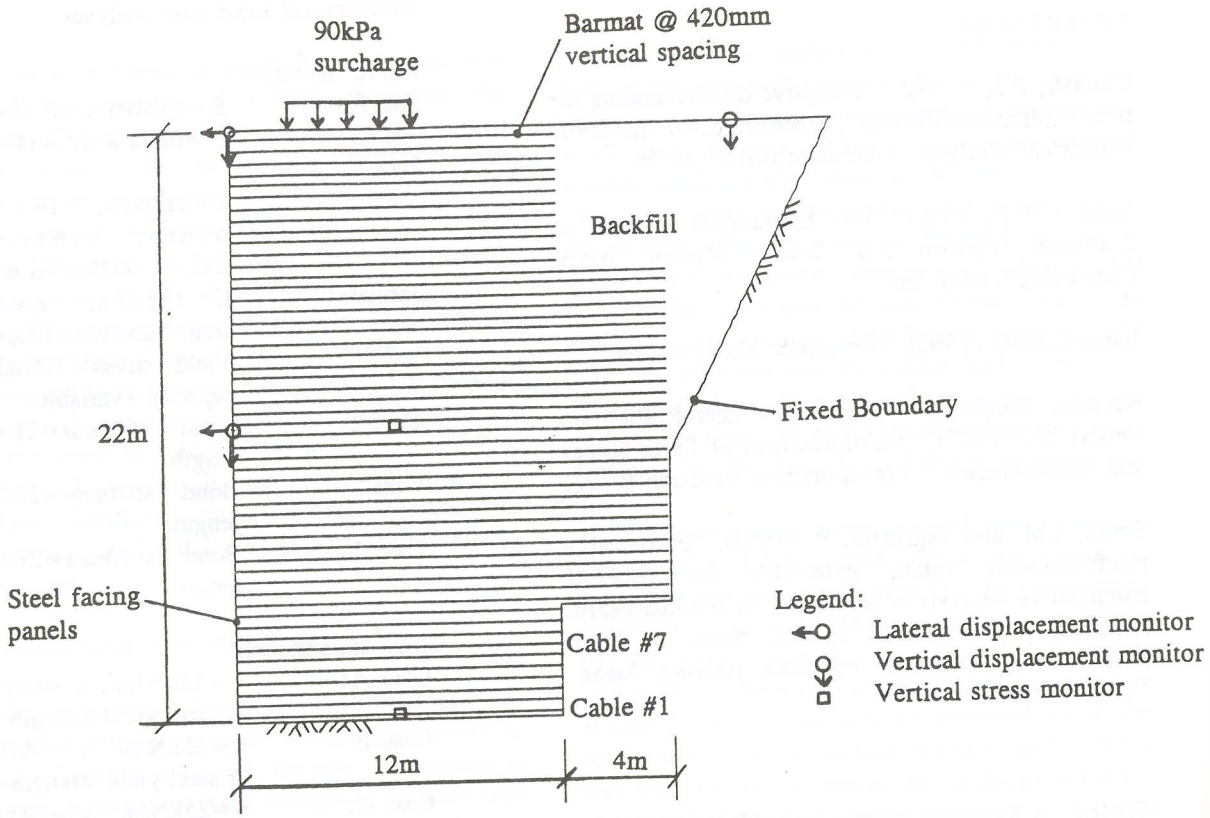

Figure 1 Reinforced soil wall model.

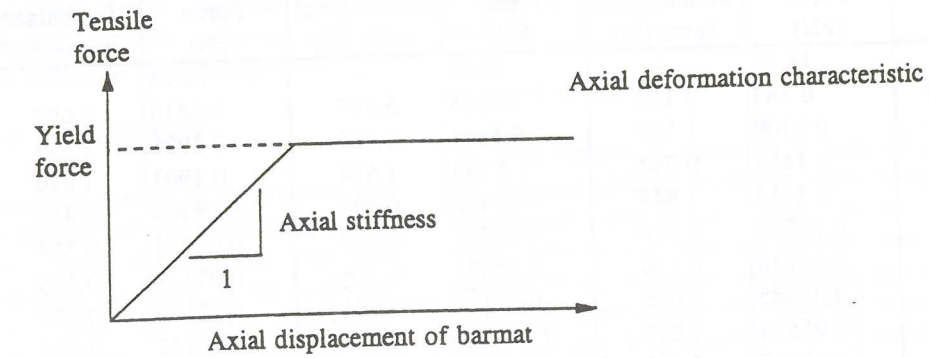

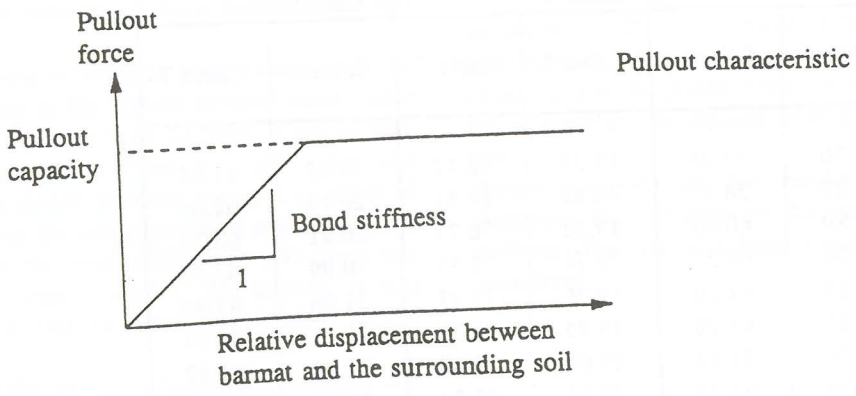

Figure 2 Idealised reinforcement behaviours.

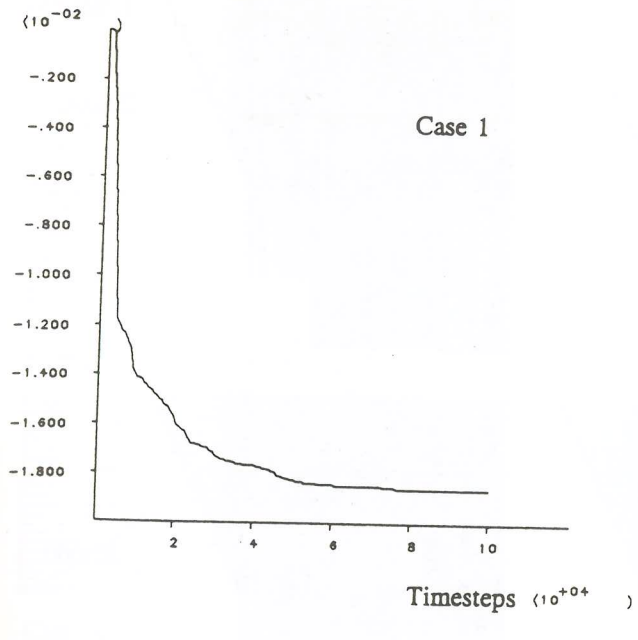

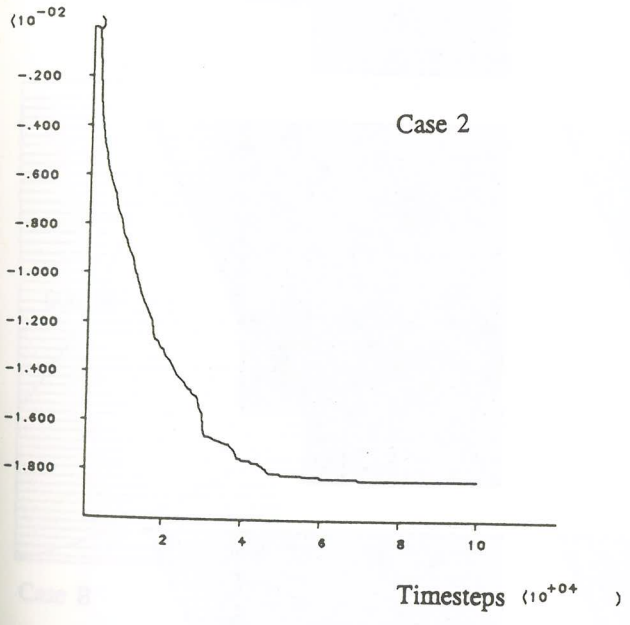

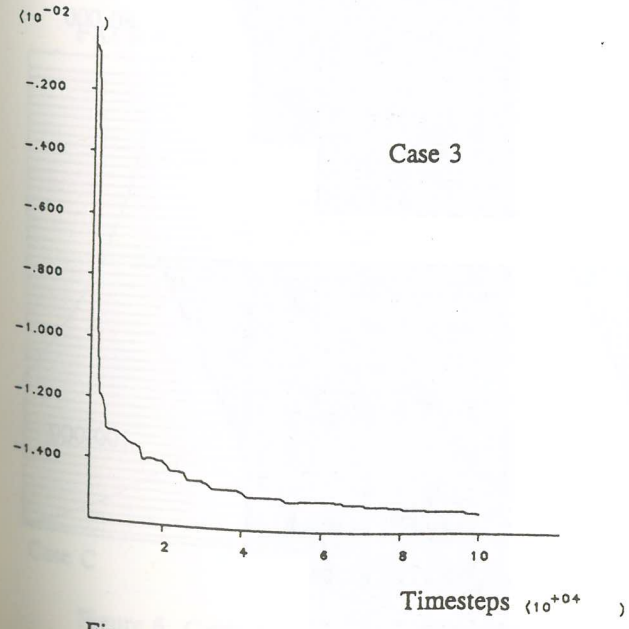

Figure 3 Plots of wall crest lateral displacement (m) with timesteps.

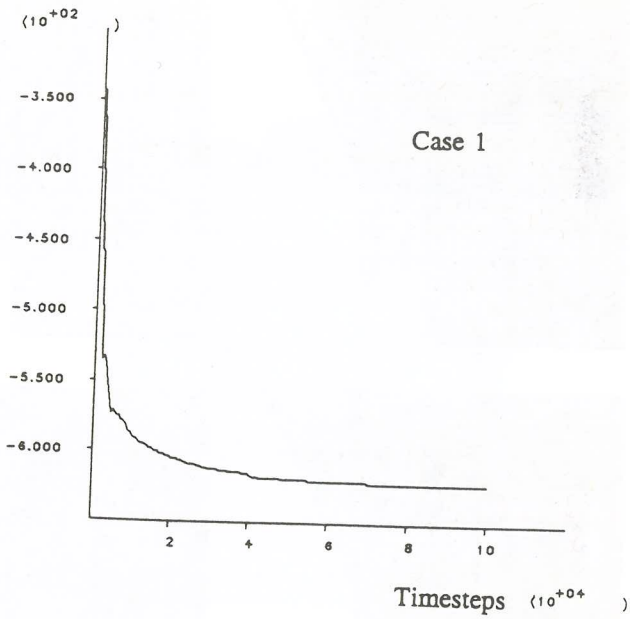

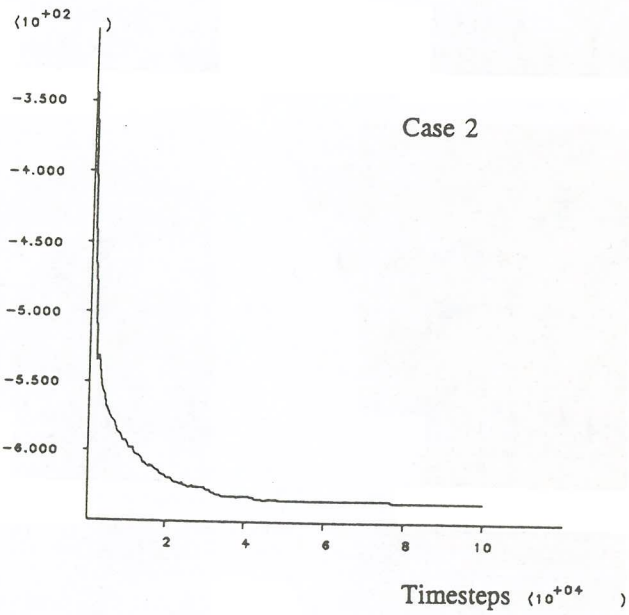

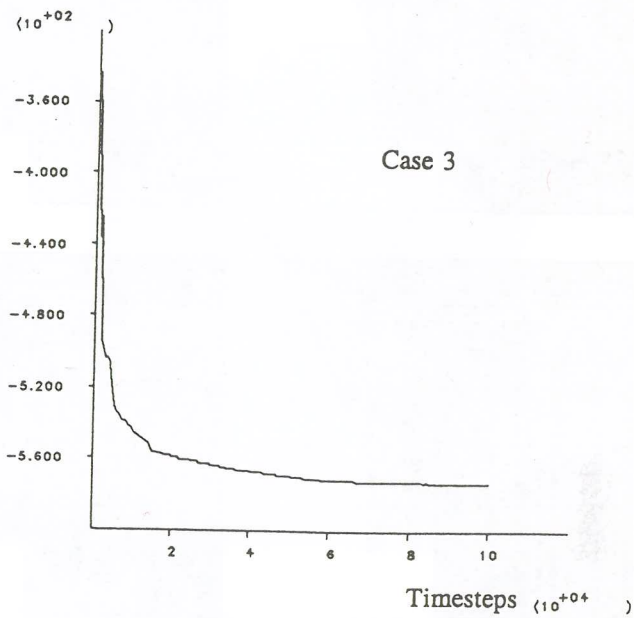

Figure 4 Plots of vertical stress (kPa) with timesteps.

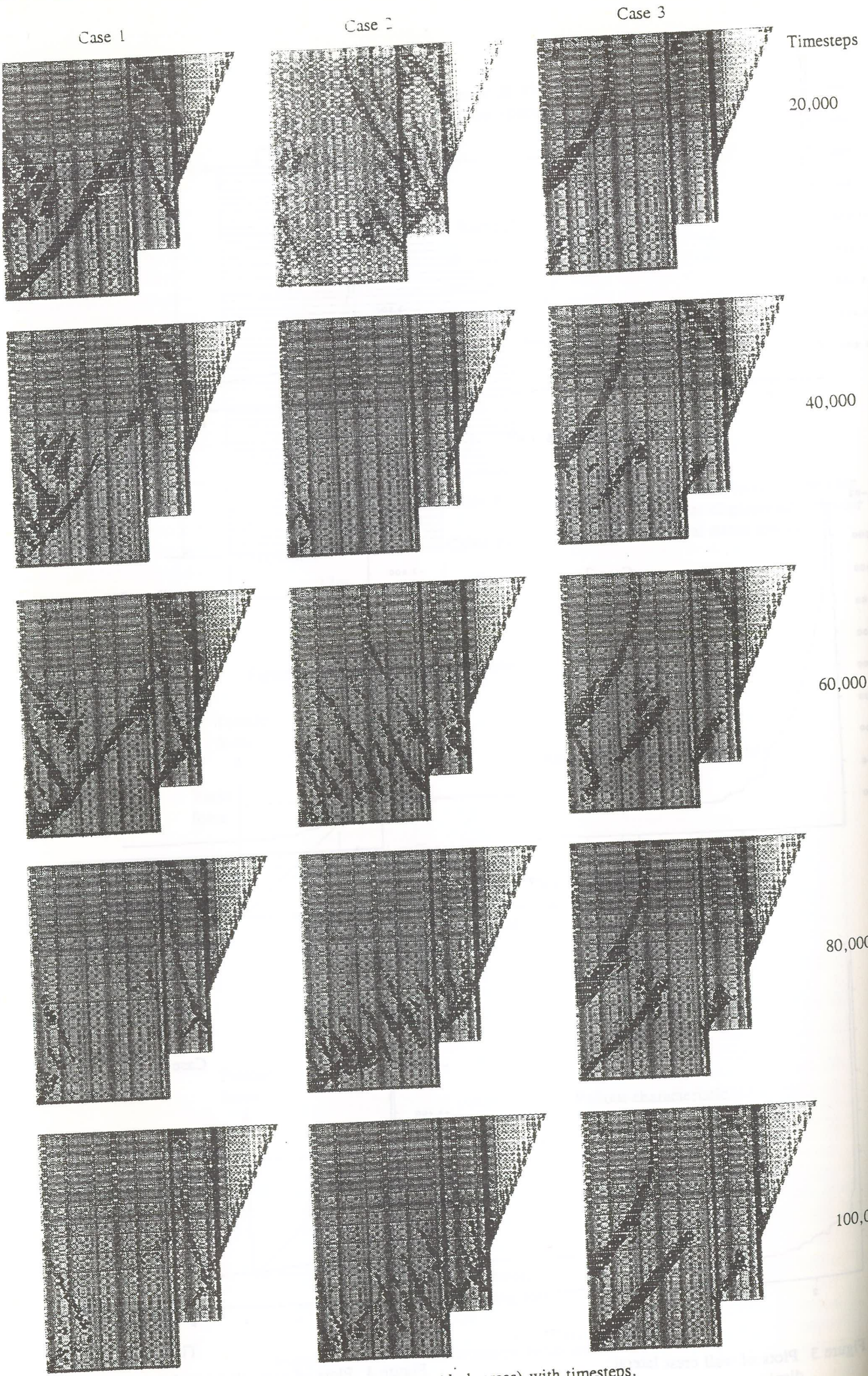

Figure 5 Development of plastic zones (dark areas) with timesteps.

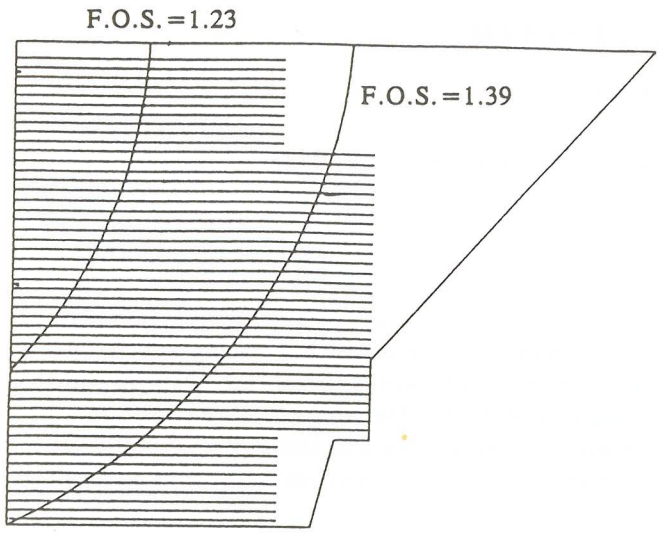

Case A

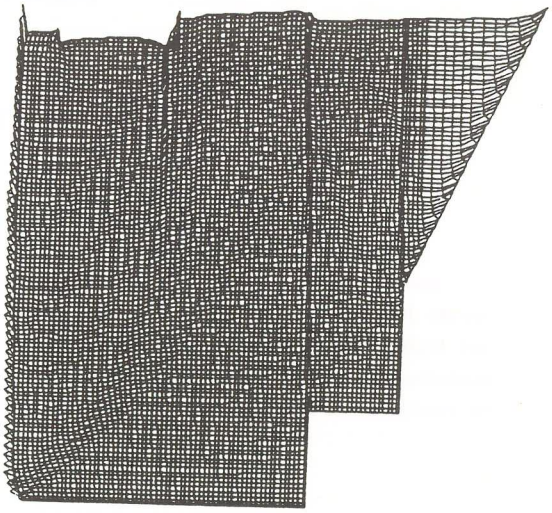

Case 1

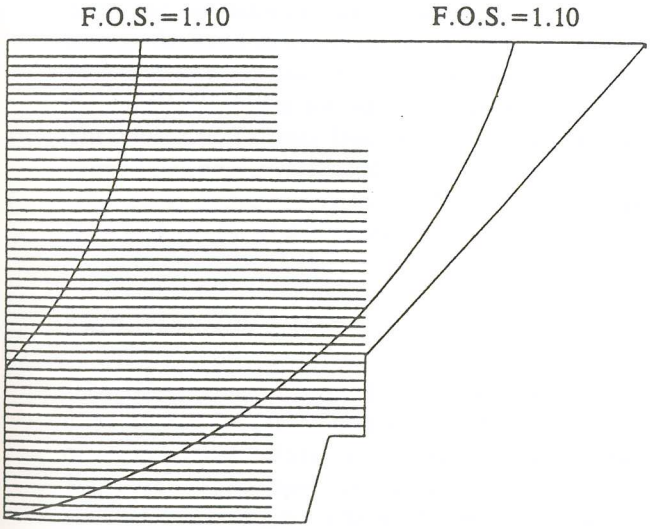

Case B

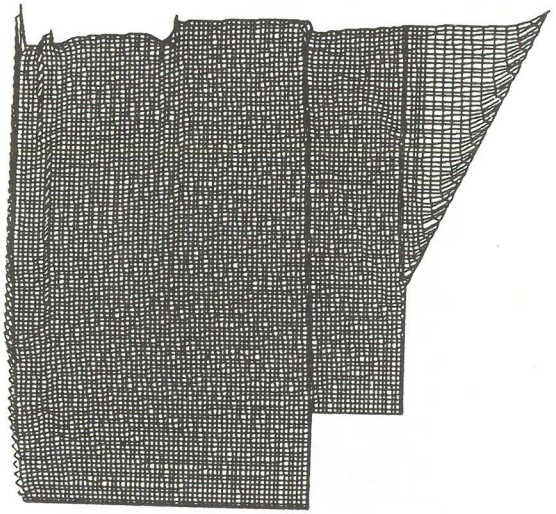

Case 2

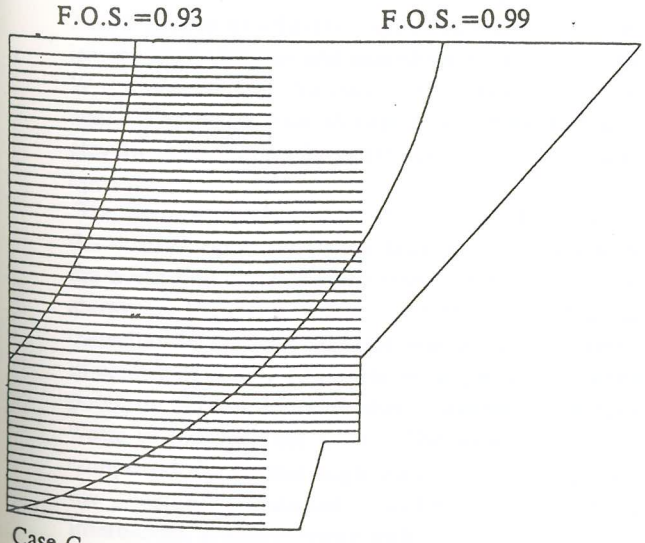

Case C

Figure 6 Critical circles predicted by the conventional limit state model.

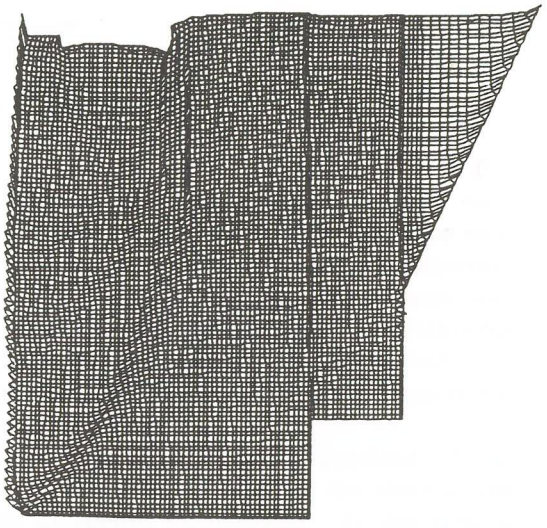

Case 3

Figure 7 Exaggerated deformation plots.